

Dielectric relaxation in chevron surface stabilized ferroelectric liquid crystals

W. Jeżewski, W. Kuczyński, and J. Hoffmann
*Institute of Molecular Physics, Polish Academy of Sciences,
Smoluchowskiego 17, 60-179 Poznań, Poland*
(9 November 2005)

The dielectric response of surface stabilized ferroelectric liquid crystals with chevron layer structure is studied within low and intermediate frequency ranges, characteristic for collective molecular excitations. By analytically solving the dynamic equation for collective molecular fluctuations under a weak alternating electric field, it is demonstrated that chevron cells stabilized by both nonpolar and polar surface interactions undergo at medium frequencies two Debye relaxation processes, connected with two chevron slabs, on opposite sides of the interface plane. This result is confirmed, experimentally, making use of the electro-optic technique. Based on qualitative arguments supported by microscopic observations of zigzag defects at different frequencies and amplitudes of the external electric field, it is shown that, at low frequencies, the electro-optic response of chevron samples is determined by three kinds of motions of zigzag walls. The first two dynamic categories are related to collective relaxation processes at weak fields, within smectic A layers forming zigzag walls, and drift or creep motions of thick walls occurring at stronger field amplitudes. Dynamic processes of the third kind correspond to sliding of zigzag walls, which appear at yet stronger field amplitudes, but below the switching threshold.

PACS numbers: 61.30.Dk, 61.30.Gd, 61.30.Hn, 81.40.Tv

I. INTRODUCTION

Thin ferroelectric liquid crystal cells with bookshelf and chevron structures play the key role in developing high-resolution and large-area display screen technologies [1]. The main technical advantage of these systems is the possibility of high-speed electro-optic switching between bistable orientational states stabilized by surface interactions [2–7]. Consequently, studies of the dynamic behavior of surface stabilized ferroelectric liquid crystals (SSFLC) have mostly been focused on ferroelectric switching processes. In the case of the chevron geometry, a challenging problem is the inclusion of the process of a rapid reorientation of molecules at the chevron interface in the theoretical description of switching phenomena [8–11]. As compared to investigations of the switching dynamics, the behavior of chevron systems in the presence of the alternating external electric field of small amplitudes, less than the switching threshold, has not been intensively studied. Collective molecular excitations generated by a weak sinusoidal applied voltage have been analyzed theoretically by solving a one-dimensional field equation describing the dynamic distribution of the azimuthal angle of the molecular c director (the projection of the molecular director on the smectic plane) with respect to the axis perpendicular to boundary plates, and then by determining the dielectric permittivity [12,13]. However, the solution to this equation has been derived by assuming an unrealistic condition that, at the chevron interface, the azimuthal angle of the c director does not depend on the external field [12,13]. Clearly, such an assumption is equivalent to the requirement that the strength of the interface anchoring interactions is infinite.

In this paper, the dynamic equation that describes collective molecular excitations in uniform symmetric SSFLC with the chevron structure under the influence of a weak sinusoidal electric field is solved for more natural interface anchoring conditions, allowing the azimuthal orientation of molecules to depend on the applied electric field also at the chevron interface. The surface interactions are assumed to include both nonpolar and polar couplings. In general, the existence of polar surface interactions, in addition to the nonpolar ones, leads to a difference in anchoring energies on two bounding plates. It is proved that the difference between the surface energies can be modified by applying the electric field across boundary plates. As will be shown, the alternating voltage induces in uniform SSFLC with bookshelf and chevron structures a nonuniform contribution to the long time average of the azimuthal angle. Such a change in the time average of molecular orientation gives rise to a variation of anchoring energies on cell plates, compared to the case of the stationary molecular orientation. It is argued here that the differentiation of effective surface energies, changed by a weak alternating voltage, causes collective relaxation processes in two slabs of uniform chevron SSFLC to run in distinct manners, with separate relaxation times. By imposing a constraint on the effective anchoring energies, these relaxation times can be interrelated. Resulting calculated dielectric loss spectra are shown to be in qualitative agreement with experimental spectra, obtained by employing the electro-optic method [14,15].

Experimental investigations of chevron SSFLC in the low-frequency regime have revealed a strong dependence of the electro-optic response on the voltage amplitude, even for small amplitudes, much less than the switching

threshold [16]. By carrying out microscopic observations and by performing measurements of the electro-optic loss, it is shown here that the low-frequency electro-optic response of chevron samples is determined by the dynamics of zigzag walls [5,17,18]. Dynamical processes occurring at very weak fields are identified with collective relaxation motions of molecules in smectic A layers, which form thin and thick zigzag walls of various sizes. It is found that, in the low-frequency regime, these motions can be described by a spectrum of Debye processes characterized by a continuous, powerlike distribution of relaxation times. The change of the low-frequency electro-optic loss as the voltage increases is attributed to the appearance of creeping motions of thick zigzag walls. Dynamic processes responsible for changes of the low-frequency electro-optic loss under further growth of the voltage are ascribed to sliding motions and gradual disappearance of zig-zag walls.

II. THEORETICAL ANALYSIS OF THE DIELECTRIC RESPONSE AT INTERMEDIATE FREQUENCIES

A. Director equation of motion

Cooperative dynamics in bookshelf and chevron cells is usually studied by analyzing fluctuations of the azimuthal angle ϕ in the smectic plane, along the surface normal direction X [4,5,12], as illustrated in Fig. 1. The contribution to the dielectric response, due to fluctuations of the angle ϕ under an applied alternating field, is usually significant in a wide range of medium frequencies. Therefore, this range is called here the intermediate frequency region. Assuming appropriate boundary conditions for the azimuthal angle, its fluctuations can be described independently in each chevron slab [4,5], by means of a dynamic field equation. In the presence of the sinusoidal external electric field applied along the X axis and alternating with the frequency ω , this equation reads

$$\frac{\partial^2 \phi}{\partial x^2} - \gamma \frac{\partial \phi}{\partial t} = A \sin \phi \cos \omega t , \quad (1)$$

where $\gamma = \gamma_\phi/K$ with γ_ϕ being the azimuthal viscosity and K being the twist elastic constant. The quantity $A = P_s E/K$ with P_s denoting the local spontaneous polarization and E being the electric field amplitude. Boundary conditions for Eq. (1) should involve preferred (zero-field) angle values at border surfaces as well as at the chevron interface. In uniform chevron cells, the c director is pretilted (in the absence of the external field) by $\pm\phi_0$, where the convention that $+$ and $-$ refer respectively to quantities on upper and lower chevron slabs is used (this convention will henceforth be adopted). Consequently, for the zero-field equilibrium state of uniform chevrons, the azimuthal angle ϕ is required here to obey the customary relation

$$\phi_\pm(0) = \mp\phi_0 , \quad (2)$$

where $\phi_\pm(0)$ refers to values of ϕ immediately above and below the interface, respectively. The amount of the pretilt ϕ_0 is, in general, nonzero and depends on the molecular and layer tilt angles and surface interaction strengths [8]. For the downward orientation of the polarization (as shown in Fig. 1), the anchoring surface energies can be supposed in the form [3,4,8,19]

$$W_\pm(\phi) = -\gamma_1 \cos^2(\phi \pm \phi_0) \pm \gamma_2 \cos(\phi \pm \phi_0) , \quad (3)$$

where γ_1 and γ_2 are respectively the nonpolar and polar surface energy strengths, the same on both bounding plates. Hence, the boundary conditions for ϕ near its zero-field equilibrium value ϕ_0 can be expressed in the case of downward-oriented chevron cells as [3,8,9]

$$\frac{\partial}{\partial x} \phi_\pm(x = \pm \frac{d}{2}) \simeq \pm v_\pm [\phi_\pm(x = \pm \frac{d}{2}) \pm \phi_0] \quad (4)$$

with d denoting the thickness of a chevron cell and

$$v_\pm = 2\lambda_1 \mp \lambda_2 \quad (5)$$

being the combined surface interactions, where $\lambda_1 = \gamma_1/K$ and $\lambda_2 = \gamma_2/K$. As the relations (4) and (5) show, the spatial derivative of ϕ depends on the combined surface interactions (taking for $\gamma_2 \neq 0$ different values at top and bottom boundary plates). For weak external fields and strong anchoring interactions at boundary and interface surfaces, one can assume, in addition to the condition (4), that [8,9]

$$\phi_\pm(\pm d/2) = \phi_\pm(0) . \quad (6)$$

In the static case ($\omega = 0$), Eq. (1) reduces to the Euler-Lagrange equation

$$\frac{\partial^2}{\partial x^2} \phi = A \sin \phi . \quad (7)$$

Using conditions (4) and (6), one finds in the case of downward oriented chevron cells in a weak constant field the following solution of Eq. (4)

$$\phi_\pm(x) = \mp\phi_0 + c f_\pm(x) + \mathcal{O}(A^2) , \quad (8)$$

where

$$f_\pm(x) = \pm \frac{A}{2} \sin \phi_0 \left(\frac{d}{2v_\pm} \pm \frac{d}{2} x - x^2 \right) . \quad (9)$$

According to Eqs. (5) and (9), the field-induced distribution of $\phi(x)$, determined by the functions f_\pm , is different in the top and bottom chevron slabs, provided that $A \neq 0$ (in particular, $|\phi_+(0)| \neq |\phi_-(0)|$). This is a result of the difference between v_+ and v_- .

For weak alternating electric fields, the solution of Eq. (1), in the case of downward polarization orientation, can be written as

$$\begin{aligned} \phi_{\pm}(x, t) = & \mp \phi_0 + b_0^{\pm} + b_1^{\pm} x \\ & + F_{\pm}(x) \cos(\omega t - \beta_{\pm}) + \mathcal{O}(A^2) , \end{aligned} \quad (10)$$

with $F_{\pm}(x)$ having series expansions

$$F_{\pm}(x) = \sum_{l=0}^{\infty} a_l^{\pm} x^l , \quad (11)$$

where β_{\pm} represents field phase shifts, different, in general, in the top and the bottom chevron slabs, b 's and a 's are spatially and temporary independent coefficients. Both b_0^{\pm} and b_1^{\pm} do not depend also on A , while $a_l^{\pm} \sim A$, $l = 0, 1, 2, \dots$. It is easy to verify that Eq. (1) has no solution of the form (10) for $b_1^{\pm} = 0$ and for any nonzero b_1^{\pm} such that $b_1^{\pm} \rightarrow 0$ as $A \rightarrow 0$. Inserting (10) into (1), equating components with the same time functions and with the spatial variable increased to the same powers, one obtains an infinite sequence of relations

$$\begin{aligned} (l+2)! a_{l+2}^{\pm} \cos \beta_{\pm} - l! \gamma \omega a_l^{\pm} \sin \beta_{\pm} &= A \rho_l^{\pm} (b_1^{\pm})^{l-2} , \\ (l+2)! a_{l+2}^{\pm} \sin \beta_{\pm} + l! \gamma \omega a_l^{\pm} \cos \beta_{\pm} &= 0 , \end{aligned} \quad (12)$$

where $l = 0, 1, 2, \dots$, and

$$\rho_l^{\pm} = \begin{cases} (-1)^{(l+2)/2} \sin(\mp \phi_0 + b_0^{\pm}) , & \text{if } l = 0, 2, 4, \dots , \\ (-1)^{(l+1)/2} \cos(\mp \phi_0 + b_0^{\pm}) , & \text{if } l = 1, 3, 5, \dots . \end{cases} \quad (13)$$

Solving Eqs. (12) with respect to the coefficients a yields

$$a_l^{\pm} = \frac{1}{l!} A \rho_l^{\pm} \cos \beta_{\pm} (b_1^{\pm})^{l-2} , \quad l = 0, 1, 2, \dots , \quad (14)$$

with

$$(b_1^{\pm})^2 = \frac{\gamma \omega}{\tan \beta_{\pm}} . \quad (15)$$

Thus, according to (13) and (14), the functions F_{\pm} can be written in a concise form as

$$F_{\pm}(x) = -A (b_1^{\pm})^{-2} \cos \beta_{\pm} \sin(\mp \phi_0 + b_0^{\pm} + b_1^{\pm} x) . \quad (16)$$

The simple form of $F_{\pm}(x)$ is a result of the occurrence of field-independent components (being a solution of the Laplace equation $\frac{\partial^2}{\partial x^2} \phi = 0$) in $\phi_{\pm}(x, t)$. The existence of these linear components in (10) implies that the long time averages $\bar{\phi}_{\pm}(x) = \lim_{T \rightarrow \infty} T^{-1} \int_0^T \phi_{\pm}(x, t) dt$ exhibit nonuniform distributions, given by $\bar{\phi}_{\pm}(x) = \mp \phi_0 + b_0^{\pm} + b_1^{\pm} x$. Such a dynamic splay is a consequence of heterogeneous, throughout chevron cells, reaction of viscosity interactions to the action of alternating electric field (note that $b_1^{\pm} \rightarrow 0$, and thereby $b_0^{\pm} \rightarrow 0$, as $\gamma \rightarrow 0$). Hence, average values of ϕ_{\pm} at boundary and interface surfaces depend not only on boundary and interface anchoring couplings but also on viscosity and elastic interactions (via γ).

Since the dynamic splay is generated by the applied alternating voltage, one can assume that, for small voltage amplitudes, this splay is not significant and hence high-order components (including coefficients a_l^{\pm} with large powers of b_1^{\pm}) in expansions (11) can be neglected. Moreover, the functions F_{\pm} should approach their static counterparts f_{\pm} as the field frequency decreases. Consequently, F_{\pm} can be approximated as

$$F_{\pm}(x) \simeq a_0^{\pm} + a_1^{\pm} x + a_2^{\pm} x^2 . \quad (17)$$

By means of relation(3), the boundary conditions for solution (10) are given now by [8,9]

$$\frac{\partial}{\partial x} \phi_{\pm}(x = \pm \frac{d}{2}, t) \simeq \mp \tilde{u}_{\pm} \mp u_{\pm} F_{\pm}(\pm \frac{d}{2}) \cos(\omega t - \beta_{\pm}) , \quad (18)$$

where

$$\tilde{u}_{\pm} = \lambda_1 \sin(2b_0^{\pm} \pm b_1^{\pm} d) \mp \lambda_2 \sin(b_0^{\pm} \pm b_1^{\pm} \frac{d}{2}) , \quad (19)$$

$$u_{\pm} = 2\lambda_1 \cos(2b_0^{\pm} \pm b_1^{\pm} d) \mp \lambda_2 \cos(b_0^{\pm} \pm b_1^{\pm} \frac{d}{2}) . \quad (20)$$

Then, imposing these boundary conditions on $\phi_{\pm}(x, t)$ and by analogy with the condition (6), using the constraint that $F_{\pm}(\pm d/2) = F_{\pm}(0)$ gives

$$b_1^{\pm} = \mp \tilde{u}_{\pm} , \quad (21)$$

$$(b_1^{\pm})^2 = \frac{4u_{\pm}}{d} , \quad (22)$$

$$\tan(\mp \phi_0 + b_0^{\pm}) = \pm \frac{4}{b_1^{\pm} d} . \quad (23)$$

Relations (22), or alternatively (21), and (23) enable one to express the constants b_0^{\pm} and b_1^{\pm} by the material parameters λ_1 , λ_2 , and ϕ_0 . Using, in turn, Eqs. (14), (22), and (23), one finds

$$F_{\pm}(x) \simeq -\frac{A}{2} \sin(\mp \phi_0 + b_0^{\pm}) \cos \beta_{\pm} (\frac{d}{2u_{\pm}} \pm \frac{d}{2} x - x^2) . \quad (24)$$

The distribution of the azimuthal angle given by the above relation is similar as in the static case [Eq. (9)], but involves modified, due to the action of the alternating electric field, *effective* combined surface interactions u_{\pm} , instead of v_{\pm} .

In the case of strong surface anchoring, one can assume that, at boundary surfaces, the effect of the dynamic splay is roughly insignificant. Then, $\bar{\phi}_{\pm}(\pm d/2) \simeq \mp \phi_0$, and hence,

$$b_0^{\pm} \simeq \mp b_1^{\pm} \frac{d}{2} . \quad (25)$$

Thus, the combined surface interactions u_{\pm} are close to v_{\pm} , respectively, for systems in weak applied fields and

with strong anchoring of molecules at surfaces. The relation (25), together with Eqs. (22) and (23), leads to an approximate relationship between λ_1 , λ_2 , and ϕ_0 . Unfortunately, this relationship is not uniquely determined, since Eqs. (23) and (25) have many solutions for a given ϕ_0 . However, instead of assuming the constraint $F_{\pm}(\pm d/2) = F_{\pm}(0)$, which refers to the static case rather than to the dynamic case, one can use the condition that the long time average of the interface energy takes its minimum value. This condition concerns the dependence of the average interface energy on the average azimuthal angle $\bar{\phi}_{\pm}(0)$. According to (25), the average azimuthal angle takes at chevron interface the values

$$\bar{\phi}_{\pm}(0) \simeq \pm\phi_0 \mp b_1^{\pm} \frac{d}{2} . \quad (26)$$

Since, in general, $b_1^+ \neq b_1^-$, the abrupt change of ϕ occurring for $E = 0$ at the interface is on average modified when the dynamic splay appears (in the presence of applied alternating field). Such a modification of the discontinuity of the average azimuthal angle at the interface is connected with an increase of the average interface energy. For chevron structures with small layer and molecular tilt angles (i.e., for typical chevron cells), the growth of the density of this energy, W_I , can be determined by

$$\varepsilon\varepsilon_0 W_I = P_s^2 - P_x^+ P_x^- + P_y^+ P_y^- , \quad (27)$$

where ε is the dielectric permittivity, whereas P_x^{\pm} and P_y^{\pm} denote x and y components of the spontaneous polarization of molecules immediately above and below the interface plane, respectively. Assuming that $|b_0^{\pm}|$ are small compared with $|\phi_0|$, allows W_I to approximate as follows

$$\varepsilon\varepsilon_0 W_I \simeq \frac{1}{2}(b_0^+ + b_0^-)^2 - \frac{1}{4}(b_0^+ b_0^-)^2 , \quad (28)$$

By minimizing W_I with respect to b_0^- (for fixed b_0^+) one gets

$$b_0^- \simeq -\frac{b_0^+}{1 - \frac{1}{2}(b_0^+)^2} . \quad (29)$$

Consequently, by virtue of (22) and (25), the above constraint yields

$$u_- \simeq \frac{u_+}{1 - du_+} . \quad (30)$$

This approximate relation is valid for systems with strong, asymmetric anchoring of molecules at bounding plates, i.e., for large γ_1 and γ_2 (in comparison to K), such that $2\gamma_1 \neq \gamma_2$. As it is shown below, it is very useful for determining the dielectric response of chevron samples.

B. Dielectric response

To determine the dynamic dielectric susceptibility and thereby the dynamic dielectric response of chevron

SSFLC, the solution (10) to Eq. (1) is applied. Thus, in the case of a sinusoidal external electric field $E(t)$ acting along the X axis, the azimuthal mode contribution to the dynamic dielectric susceptibility can be written as

$$\chi(\omega) = \lim_{E \rightarrow 0} \frac{P_s}{E(t)} [\langle \cos \phi_+(x, t) \rangle_+ - \langle \cos \bar{\phi}_+(x) \rangle_+ + \langle \cos \phi_-(x, t) \rangle_- - \langle \cos \bar{\phi}_-(x) \rangle_-] , \quad (31)$$

where $\langle \dots \rangle_{\pm}$ denote space averages over respectively upper and lower chevron arms, so that, e.g.,

$$\langle \cos \phi_{\pm}(x, t) \rangle_{\pm} = \pm \frac{2}{d} \int_0^{\pm d/2} \cos \phi_{\pm}(x, t) dx . \quad (32)$$

Using Eqs. (10), (22)-(25), and (31), and assuming that $|b_0^{\pm}|$ are small, one derives

$$\frac{\chi(\omega)}{\varepsilon_0} = \varepsilon'(\omega) + \varepsilon''(\omega) \tan(\omega t) , \quad (33)$$

with the dielectric permittivity

$$\varepsilon'(\omega) = B(\cos^2 \beta_+ + \cos^2 \beta_-) \quad (34)$$

and the dielectric loss permittivity

$$\varepsilon''(\omega) = B(\tan \beta_+ \cos^2 \beta_+ + \tan \beta_- \cos^2 \beta_-) , \quad (35)$$

where

$$B = \frac{Ad}{4u_+} \sin^2 \phi_0 . \quad (36)$$

By means of Eqs. (15) and (22), the phase shifts $\beta_{\pm} = \omega\tau_{\pm}$ with the relaxation times

$$\tau_{\pm} = \frac{\gamma d}{4u_{\pm}} . \quad (37)$$

Hence, the dielectric response of chevron cells stabilized by both nonpolar and polar surface interactions can be described in the case of weak applied electric field by two Debye processes. These processes are determined by different relaxation times, each characterizing collective motions of molecules on opposite sides of the chevron interface. Making use of relation (30), valid for systems that display strong anchoring of molecules at bounding surfaces, one can describe the dielectric response of chevron samples by three parameters: B , τ_+ (or equivalently τ_-), and d . Moreover, having determined the relaxation times, one obtains the parameters γ , u_+ , and u_- . A simple method to calculate the combined surface interactions u_+ and u_- , based on experimental data, is described below.

C. Calculation of surface energy parameters

The permittivity spectra (34) and (35) involve two Debye relaxation processes with equal strengths. In such a case, the loss permittivity possesses a single maximum if the ratio $\nu = \tau_+/\tau_-$ is $\nu \geq \nu_c$, where $\nu_c = 3 - 2\sqrt{2} \approx 0.172$, and two maxima of equal heights if $\nu < \nu_c$. However, the case of the double maximum form of $\varepsilon''(\omega)$ is not considered here because typical experimental loss permittivity spectra obtained for chevron cells do not display equal, or nearly equal, maxima that could be ascribed to collective azimuthal excitations of molecules.

In order to compare theoretical [Eqs. (34) and (35)] and experimental spectra $\varepsilon(\omega)$, one has to determine combined surface interactions u_{\pm} . By applying the approximate relation (30), one can describe $\varepsilon(\omega)$ by one energy parameter, say u_+ . Then, the position of the maximum of $\varepsilon''(\omega)$ is given by

$$\omega_{\max}\tau_+ = 1/\sqrt{\nu} , \quad (38)$$

where $\nu = 1 - du_+$. For a value of ω_{\max} found experimentally, this relation enables one to express the relaxation time τ_+ by u_+ and the cell thickness d . Next, introducing the rates $\eta(\omega) = \varepsilon'(\omega)/\varepsilon''(\omega)$ and $\sigma(\omega) = \omega/\omega_{\max}$, and applying (34) and (35), leads to the following biquadratic equation with respect to ν :

$$\sigma^2 p^2 - \eta\sigma(1 + \sigma^2)p + 2(1 - \sigma^2) = 0 \quad (39)$$

with

$$p = \nu + \frac{1}{\nu} . \quad (40)$$

As a result, solving Eq. (39) for different values of ω and for respective, experimentally obtained values of η , yields u_+ as a function of ω . Since u_+ is essentially independent of ω , this function should be constant or should at least exhibit a plateau in some range of frequency. Thus, the considered procedure enables one not only to determine the surface energy parameter u_+ , but also to test the above theoretical description of the dielectric response of chevron systems. In particular, one can determine the frequency region where this description is valid.

III. EXPERIMENTAL

To verify the presented theory, dielectric measurements on the liquid-crystalline mixture Felix 15-100, commercially available from Clariant have been carried out. The investigated mixture exhibits ferroelectric smectic C* phase at room temperature and transforms into the paraelectric smectic A phase at 73 °C. The measurements presented in this paper were performed at temperature 50 °C, i.e., 23 °C below the ferroelectric-paraelectric phase transition. The investigated material was introduced into

commercially available measuring cells of various thicknesses (5 μm , from Linkam, UK, and 12.1 μm , 25.9 μm , 50 μm , from EHC, Japan). The thickness of all cells used was less than or comparable to the helical pitch of the investigated material ($\sim 20 \mu\text{m}$), thus the chevron texture was easily attained. The walls of measuring cells were provided with indium-tin-oxide (ITO) semitransparent electrodes coated with thin polymer layers. These layers were rubbed unidirectionally along antiparallel directions on both plates. This promoted the orientation of molecules more or less parallel to electrodes and reduced the ionic current flowing across the sample. The measuring cell was placed inside a modified Mettler hot stage, in which the temperature was controlled using a Digi-Sense temperature controller. The hot stage was installed between crossed polarizers of a polarizing microscope (Biolar, from PZO, Poland). The angle between the polarization plane of the incident light and the optic axis of the sample in the smectic A phase was set to 22.5°. The intensity of light passing the sample and polarizers was registered using a photodiode connected to a preamplifier and lock-in amplifier SR 850 from Stanford Research (USA). Simultaneously, the electric capacitance of the sample was measured using the Hewlett-Packard low-frequency impedance analyzer HP 4192A. The measurements indicated that the dielectric increment (the difference between the electric permittivity in the smectic C* phase and in the smectic A phase) was exactly proportional to the light modulation depth, detected by the photodiode, as it was already demonstrated in Ref. [20]. Thus, the dielectric measurements might be well replaced by electro-optic measurements, which are more accurate. Moreover, they are less sensitive to ionic current, especially at low frequencies [20]. This property enabled one to extend the measurement range down to ~ 10 Hz. In this way, reliable results were obtained at much lower frequencies than it might be possible using typical dielectric methods. Therefore, in what follows, electro-optic experimental results obtained for frequencies greater than 10 Hz are only discussed.

IV. RESULTS AND DISCUSSION

The approach developed here to analyze the dielectric response of SSFLC with chevron geometry requires determining the effective surface interaction u_+ . Using electro-optic data obtained for samples of different thicknesses and employing the procedure of Sec. II C, the parameter u_+ has been derived as a function of frequency in cases of various values of the voltage amplitude U . Plots of u_+ are shown in Fig. 2 for a low voltage, $U = 0.1$ V. It is seen that, for samples of different thicknesses, u_+ remains nearly constant within rather wide frequency ranges, and quickly decreases outside these ranges. Clearly, the rapid decay of u_+ in the low-frequency region is a consequence of an overlapping,

in the dielectric response, between contributions arising from collective azimuthal excitations of molecules in chevron slabs and contributions that have other origins than these collective excitations. Similarly, a less sudden downfall of u_+ in high-frequency regions can be ascribed to components of $\varepsilon(\omega)$ corresponding to high-frequency processes [21], separated to a large extent from the collective processes occurring at intermediate frequencies. Naturally, the region of frequencies for which the parameter u_+ remains approximately constant determines the range of the validity of the introduced theoretical approach.

The surface energy parameter u_+ has been found for cells of different thicknesses by averaging parameter values calculated for frequencies belonging to ranges in which these values are nearly constant. Results of calculations of u_+ for $U = 0.1$ V are given in Table I, where corresponding values of the ratio ν and the frequency $f_{\max} = \omega_{\max}/2\pi$ are also given. Values of u_+ determined for various voltages demonstrate that u_+ scarcely depends on the voltage amplitude if U remains relatively small, below some value U_{lin} , different, in general, for individual samples ($U_{\text{lin}} \approx 3$ V for studied samples of the thickness $d = 5$ μm). When the voltage amplitude exceeds this value, nonlinear effects in $\varepsilon(\omega)$ become significant and Eq. (39) loses real, positive solutions for medium frequencies. As is seen from Table I, values of ν , obtained in the low-voltage regime, are much greater than the threshold value, above which $\varepsilon''(\omega)$ has a single maximum. This means that, for the investigated SSFLC samples, differences between anchoring energies on both boundary plates do not strongly affect the form of the function $\varepsilon''(\omega)$. The dielectric response of studied chevron cells displays a dependence on the sample thickness. In particular, f_{\max} decreases and thereby both the relaxation times τ_{\pm} increase, as d grows. The increase of τ_{\pm} with d is a consequence of a stabilization of collective reorientations of molecules by strong surface interactions. Since these interactions force the molecular ordering in entire chevron cells, time needed to reach the ordered state in initially perturbed samples is longer and longer as d grows and/or as the surface interactions become weaker. This is consistent with relation (37). Clearly, the dependence of the effective surface interactions u_{\pm} on the sample thickness (as seen in Fig. 2 in the case of u_+) originates, in general, from the dependence of surface energy strengths γ_1 and/or γ_2 on d . However, to explain such a behavior of γ_1 or γ_2 as d is varied, one would analyze dynamic processes leading to the appearance of surface interactions.

To test the method introduced here for investigating dielectric response of chevron cells, dielectric spectra have been determined using Eqs. (30), (34), (35), (37), and (38) with values ω_{\max} and $\varepsilon''(\omega_{\max})$ found experimentally. Additionally, a simple relaxation model that involves a single Debye process, characterized by the same values of ω_{\max} and $\varepsilon''(\omega_{\max})$, has been considered. Both resulting theoretical dielectric loss spectra as well

as experimental spectra obtained for the voltage amplitude $U = 0.1$ V are plotted in Fig. 3 for intermediate frequencies. These plots show that the experimentally determined dielectric loss spectra exhibit a broadening near their maxima, compared to corresponding spectra obtained for single Debye relaxation processes, and that such a broadening is well described by the introduced model including two Debye processes. Consequently, the effect of smearing of $\varepsilon''(\omega)$ near its maximum, located in the intermediate frequency region, can be considered as a result of a difference between anchoring energies at boundary surfaces. However, when ω decreases starting from ω_{\max} , there appears a discrepancy between measured and theoretically predicted dielectric loss permittivities, as illustrated in Fig. 4. This inconsistency is due to the occurrence in chevron samples of molecular motions other than the collective molecular reorientations taken into account in the theoretical model. Such additional motions are called here low-frequency processes, although they markedly affect the spectra $\varepsilon(\omega)$ even for ω relatively close to ω_{\max} . Thus, frequency regions, in which low- and medium-frequency processes are significant, are not quite separated, and a rigid determination of the corresponding low- and intermediate-frequency ranges is not possible.

To interpret the complicated low-frequency behavior of the dielectric loss permittivity, it has been suggested that various dynamic mechanisms can be of importance in low-frequency regime [16,22]. However, no detailed analysis of the complex dielectric response of chevron cells at low frequencies has been reported yet. For low voltages (for which the dielectric response is linear) contributions to $\varepsilon(\omega)$ that arise from dynamic processes other than fluctuations of the azimuthal angle with chevron slabs can easily be investigated by a subtraction of theoretical functions $\varepsilon_t(\omega)$ involving two relaxation times from respective experimental spectra $\varepsilon_e(\omega)$. Resulting extracted loss spectra $\Delta\varepsilon'' = \varepsilon_e'' - \varepsilon_t''$ are shown in Fig. 5 for samples of different thicknesses, in the case of $U = 0.1$ V. It proves that, for each system under study here, $\Delta\varepsilon''$ has a single maximum at a frequency ω_0 of the same order of magnitude. Evidently, $\Delta\varepsilon''$ displays for $\omega > \omega_0$ a complex form, different from the shape of loss spectra corresponding to single Debye processes or even to sums of a few single processes. This suggests that the dielectric response of chevron cells can approximately be described by a spectrum of Debye processes with a continuous distribution of relaxation times. Then, for low frequencies, such that $\omega \geq \omega_0$, the extracted loss permittivity can be expressed as

$$\Delta\varepsilon''(\omega) = \frac{1}{\omega} \int_{\tau_1}^{\tau_2} \rho(\tau) \frac{\omega\tau}{1 + \omega^2\tau^2} d\tau, \quad (41)$$

where $\tau_2 \leq 1/\omega_0$ and τ_1 are respectively maximal and minimal relaxation times, and $\rho(\tau)$ denotes the distribution of relaxation times. For $\omega \geq \omega_0$, the shape of the extracted spectra determined with the use of experimental data can easily be recovered by assuming that

$$\rho(\tau) \sim \tau^{-2} . \quad (42)$$

Thus, applying (41) and (42) yields

$$\Delta\varepsilon''(\omega) = C_1 \ln \left[\frac{\tau_2^2(1 + \omega^2\tau_1^2)}{\tau_1^2(1 + \omega^2\tau_2^2)} \right] \quad (43)$$

with C_1 being a positive constant. Similarly, using (42), one finds the extracted dielectric permittivity $\Delta\varepsilon'$ to be

$$\Delta\varepsilon'(\omega) = C_2 \left[\frac{1}{\omega} \left(\frac{1}{\tau_1} - \frac{1}{\tau_2} \right) - \arctan(\omega\tau_2) + \arctan(\omega\tau_1) \right] , \quad (44)$$

where C_2 denotes a constant. Results of fits of functions given by Eqs. (43) and (44) (on adjusting the parameters C_1 , C_2 , τ_1 , and τ_2) to respective extracted spectra obtained with the use of experimental data are shown in Figs. 5 and 6. It is seen that the agreement between postulated and experimental extracted spectra $\Delta\varepsilon''$ is good (as long as $\omega \geq \omega_0$), but is less satisfactory in the case of the spectra $\Delta\varepsilon'$. Nevertheless, these figures demonstrate that the low-frequency dielectric response of chevron cells can indeed be characterized by Debye processes with continuously distributed relaxation times. It should also be noted that the measured spectra presented in Fig. 5, contrary to earlier results derived from a numerical decomposition of the dielectric loss spectra [13], do not reveal the existence of any contributions that would correspond to surface fluctuations of the c director (at frequencies of an order magnitude greater than ω_{\max}).

Turning to observations of chevron samples through polarizing optical microscope, it is argued here that a complex dielectric response of SSFLC is connected to dynamics of zigzag defects [1]. Usually, these defects appear spontaneously, forming irregular patterns, when chevron cells are cooled down [1,4,18,23,24]. Microscopic observations of chevron samples performed in the low-frequency regime at weak voltages have displayed periodic changes (according to a voltage alternation) of the color and the intensity of light transmitted not only by uniform chevron regions (domains) but also by thin and thick zigzag walls separating these regions, as illustrated in the microphotographs of Fig. 7 for a sample of the thickness $d = 5 \mu\text{m}$. Thus, in addition to uniform domains, collective relaxation processes caused by a weak voltage alternating with low frequencies occur also inside zigzag walls of different widths. Since zigzag walls reveal various shapes as well as sizes [1,17,18] and consist of smectic A layers having different thicknesses, Consequently, being affected by surface interactions with different strengths, one can infer that relaxation times characterizing dynamic processes within these walls undergo a nonuniform distribution. Then, the complexity of the dielectric response of chevron cells to weak voltages alternating with low frequencies may, in fact, be considered as a result of relaxation processes within zigzag walls.

As the amplitude of the applied voltage exceeds a threshold U_1 (different, in general, for various samples),

thick zigzag walls start to creep. Such a drift viscous motion of defect walls, induced by an alternating electric field, is spatially confined by pinning ends of thick walls to ends of thin walls. This is illustrated in Fig. 8 for the same sample of the width $d = 5 \mu\text{m}$, in the case of the voltage amplitude $U = 1.0 \text{ V}$ and the frequency $f = 100 \text{ Hz}$. The drift motion of thick walls [Figs. 8(a) and 8(b)] is not periodic, although long time averages of displacements $r(t)$ of these walls vanish, i.e., $\lim_{t \rightarrow \infty} r(t) = 0$, as shown in Fig. 8(c).

When the voltage amplitude goes beyond another threshold U_2 ($U_2 > U_1$), both thin and thick walls begin to slide. Such irreversible motions of zigzag walls are accompanied with a gradual shrinkage of corresponding zigzag lines on boundary surfaces and with gradual disappearing of the defect walls, as U grows, remaining below the switching threshold U_s . Thus, the density of zigzag defects decreases when U grows (above the sliding threshold U_2). The effect of motions of zigzag walls in the sliding regime is presented in Fig. 9 for the studied sample of the thickness $d = 5 \mu\text{m}$, in the case of the voltage amplitude $U = 5 \text{ V}$ and the frequency $f = 100 \text{ Hz}$. Note that the threshold voltage at which the switching process appears, found for samples of different thicknesses, increases with d (e.g., $U_s = 10 \text{ V}$ for the case of $d = 5 \mu\text{m}$, while $U_s = 20 \text{ V}$ for the case of $d = 25.9 \mu\text{m}$). Analysis of the dynamics of defects presented here indicates that both the threshold voltages U_1 and U_2 (similarly to U_s) are different for samples of different thicknesses. However, to answer the question of whether the dependence of these threshold voltages on the sample thickness has a general character, and to possibly determine such a general dependence, further work on a wider class of uniform chevron cells is needed.

Changes in the dynamic behavior of defect walls as U crosses its threshold values are markedly reflected in the low-frequency dielectric loss spectra, as illustrated in Fig. 10. It is seen that, in comparison to relaxation processes inside zigzag walls, creep motions of thick walls give a large contribution to $\varepsilon''(\omega)$, in almost the entire low-frequency range, with a distinct maximum. Contrary to creep loss spectra, sliding spectra (associated with sliding of defect walls) have very small amplitudes for $f > 10 \text{ Hz}$. This is a consequence of the fact that sliding motions are very slow compared to creep motions. Hence, the dielectric loss is dominated in the sliding regime by the low frequency tail of contributions to $\varepsilon''(\omega)$ arising from collective fluctuations of the azimuthal orientation of the c director. It should be noted that similar relaxation, creep, and slide motions of complex objects in elastic media have recently been studied, both theoretically and experimentally, in various contexts. In particular, thermally activated and/or field-induced domain wall motions of these types have been investigated in impure magnets [25], polydomain relaxor-ferroelectric single crystals [26], discontinuous metal-insulator multilayer systems [27], and periodically poled ferroelectric single crystals [28]. Transitions between different dy-

dynamic states of domain walls occurring in these systems have been shown to reveal a character of dynamic phase transitions, at critical field amplitudes being some functions of the temperature T and the frequency of the field alternation. Clearly, one can expect that changes in the dynamics of zigzag walls appearing in chevron SSFLC also display a character of dynamic phase transitions, determined in the parameter space $(U - T - \omega)$. A detailed exploration of this question is, however, beyond the scope of this paper.

V. CONCLUSIONS

It has been shown in this paper that the dielectric response of ferroelectric chevron systems stabilized by nonpolar and polar surface interactions is determined at intermediate frequencies by two Debye relaxation processes, corresponding to collective fluctuations of the azimuthal orientation of molecules in two chevron slabs. This relaxation mechanism has been proved to cause a broadening of the dielectric loss spectrum near its maximum, compared to a spectrum obtained for a model involving a single Debye process. Such a broadening effect has been confirmed experimentally, for chevron cells of different thicknesses. To investigate low-frequency processes and possible intermediate-frequency processes, other than cooperative fluctuations of azimuthal orientations of the c director, theoretically derived dielectric response functions have been extracted from respective measured electro-optic spectra. Resulting extracted spectra have not displayed any additional processes at medium frequencies, even for relatively thick samples. This is in contrast to an earlier suggestion [13] that, in a medium-frequency region, the dielectric response of thick enough cells can be affected by surfacelike fluctuations of the c director. It has been demonstrated that low-frequency dynamic processes have different character in three voltage regimes and can be ascribed to relaxation processes inside thin and thick zigzag walls, creeping of thick walls, and sliding as well as disappearing of defect walls. Certainly, low-frequency dielectric response of chevron cells can be affected by other kinds of defects or smectic layer deformations [1,23,29]. However, the low-frequency dynamic mechanisms discussed in this paper appear to be most important. Finally, it should be remarked that the possibility of macroscopic observations of dynamic behaviors of defect walls provides a useful tool of studying low-frequency dynamic states of chevron SSFLC and dynamic phase transitions between these states.

ACKNOWLEDGMENTS

The authors are very grateful to J. Małeckı for useful discussions. This work was supported by Polish Research

Committee (KBN) under grant No. 2PO3B 127 22.

-
- [1] S.T. Lagerwall, *Ferroelectric and Antiferroelectric Liquid Crystals* (Wiley-VCH, Weinheim, 1999).
 - [2] N.A. Clark and S.T. Lagerwall, *Appl. Phys. Lett.* **36**, 899 (1980).
 - [3] M.A. Handschy, N.A. Clark, and S.T. Lagerwall, *Phys. Rev. Lett.* **51**, 471 (1983).
 - [4] M.A. Handschy and N.A. Clark, *Ferroelectrics* **59**, 69 (1984).
 - [5] T.P. Rieker, N.A. Clark, G.S. Smith, D.S. Parmar, E.B. Sirota, and C.R. Safinya, *Phys. Rev. Lett.* **59**, 2658 (1987).
 - [6] J. Xue, N.A. Clark, and M.R. Meadows, *Appl. Phys. Lett.* **53**, 2397 (1988).
 - [7] D. Coleman, D. Mueller, N.A. Clark, J.E. MacLennan, R.-F. Shao, S. Bardon, and D.M. Walba, *Phys. Rev. Lett.* **91**, 175505 (2003).
 - [8] J.E. MacLennan, N.A. Clark, M.A. Handschy, and M.R. Meadows, *Liq. Cryst.* **7**, 753 (1990).
 - [9] J.E. MacLennan, M.A. Handschy, and N.A. Clark, *Liq. Cryst.* **7**, 787 (1990).
 - [10] C.R. Brown, P.E. Dunn, and J.C. Jones, *Eur. J. Appl. Math.* **8**, 281 (1997).
 - [11] L.D. Hazelwood and T.J. Sluckin, *Liq. Cryst.* **31**, 683 (2004).
 - [12] Y.P. Panarin, Yu.P. Kalmykov, S.T. MacLughadha, H. Xu, and J.K. Vij, *Phys. Rev. E* **50**, 4763 (1994).
 - [13] O.E. Kalinovskaya, J.K. Vij, Y.V. Tret'yakov, and Y.P. Panarin, *Liq. Cryst.* **26**, 717 (1999).
 - [14] P. Pierański, E. Guyon, P. Keller, L. Liebert, W. Kuczyński, and P. Pierański, *Mol. Cryst. Liq. Cryst.* **38**, 275 (1977).
 - [15] W. Kuczyński, J. Hoffmann, and J. Małeckı, *Ferroelectrics* **150**, 279 (1993).
 - [16] Y.P. Panarin, H. Xu, S.T. MacLughadha, and J.K. Vij, *Jpn. J. Appl. Phys.* **33**, 2648 (1994).
 - [17] N.A. Clark and T.P. Rieker, *Phys. Rev. A* **37**, 1053 (1988).
 - [18] L. Limat, *Europhys. Lett.* **44**, 205 (1998).
 - [19] M. Nagakawa, M. Ishikawa, and T. Akahane, *Jpn. Appl. Phys.* **27**, 456 (1988).
 - [20] W. Kuczyński, in *Relaxation Phenomena, Liquid Crystals, Magnetic Systems, Polymers, High T_c -Superconductors, Metallic Glasses*, edited by W. Haase and S. Wróbel (Springer, New York, 2003).
 - [21] F. Gouda, K. Skarp, and S.T. Lagerwall, *Ferroelectrics* **113**, 165 (1991).
 - [22] S. Havrilak Jr., J.K. Vij, and M. Ni, *Liq. Cryst.* **26**, 465 (1999).
 - [23] A. Fukuda, Y. Ouchi, H. Arai, H. Takano, K. Ishikawa, and H. Takezoe, *Liq. Cryst.* **5**, 1055 (1989).
 - [24] C. Wang, R. Kurihara, P.J. Bos, and S. Kobayashi, *J. Appl. Phys.* **90**, 4452 (2001).
 - [25] T. Nattermann, V. Pokrovsky, and V.M. Vinokur, *Phys.*

Rev. Lett. **87**, 197005 (2001).

- [26] W. Kleemann, J. Dec, S. Miga, Th. Woike, and R. Pankrath, Phys. Rev. B **65**, 220101(R) (2002).
 [27] X. Chen, O. Sichelschmidt, W. Kleemann, O. Petravic, Ch. Binek, J.B. Sousa, S. Cardoso, and P.P. Freitas, Phys. Rev. Lett. **89**, 137203 (2002).
 [28] Th. Braun, W. Kleemann, J. Dec, and P.A. Thomas, Phys. Rev. Lett. **94**, 117601 (2005).
 [29] N. Ul Islam, N.J. Mottram, and S.J. Elston, Liq. Cryst. **26**, 1059 (1999).

FIG. 1. Geometry of orientation states in a uniform chevron cell of thickness d : (a) in the smectic layer plane (X - Y), and (b) in the (X - Z) plane (perpendicular to the smectic layer plane and to the bounding plates). In (a) the symbols \rightarrow and \vdash represent, respectively, projections of the microscopic polarization \vec{P}_s and the c director \vec{c} on the plane (X - Y). In (b) the symbols \rightarrow and $>-$ denote respectively projections of \vec{P}_s and the molecular director \vec{n} on the plane (X - Z). Scales of projections of vectors \vec{c} and \vec{n} on the planes (X - Y) and (X - Z), respectively, are not preserved. The abbreviations T and B indicate top and bottom bounding surfaces, respectively, whereas I denotes the interface plane. The azimuthal angle ϕ takes pretilt values $\phi = \pm\phi_0$ in upper and lower chevron slab, respectively.

FIG. 2. The surface interaction parameter u_+ determined as function of the frequency of the alternating voltage of the amplitude $U = 0.1$ V, for samples of different thicknesses: $d = 5$ μm (\circ), $d = 12.1$ μm (\triangle), $d = 25.9$ μm (\square).

FIG. 3. Loss spectra determined experimentally (dots) within a medium frequency range, for $U = 0.1$ V, in cases of chevron cells of thicknesses $d = 5$ μm and $d = 12.1$ μm , and derived theoretically by the use of the approach including two Debye processes (labeled 1) as well as by the use of the single relaxation model (labeled 2). Theoretical plots were obtained for respective, measured values of ω_{max} and $\varepsilon''(\omega_{\text{max}})$.

FIG. 4. Experimental (dots) and theoretical (solid lines) loss spectra for chevron cells of different thicknesses. Theoretical plots were obtained by the use of the approach involving two Debye processes.

FIG. 5. Dielectric loss spectra obtained by a subtraction of theoretical loss spectra ε_t from experimental spectra ε_e , in cases of samples of different thicknesses, for $U = 0.1$ V. Dots correspond to experimental data, while the solid line refers to the postulated function of Eq. (43).

FIG. 6. Extracted spectra $\Delta\varepsilon'$ obtained for a sample of the thickness $d = 5$ μm , in the case of $U = 0.1$ V. Dots refer to experimental data and the solid line represents the function given by Eq. (44).

FIG. 7. (Color online) Zigzag walls in a chevron cell of the thickness $d = 5$ μm , under the influence of a voltage of the amplitude $U = 0.5$ V, alternating with the frequency $f = 10$ Hz. The microphotographs were taken at a short time period, both at the speed shutter 1/100 s. These micrographs give an evidence of a pulsation of light transmitted not only by domains but also by defect walls of various widths.

FIG. 8. (Color online) Creep motions of thick zigzag walls in a sample of the thickness $d = 5$ μm , induced by an alternating voltage of the amplitude $U = 1$ V and the frequency $f = 100$ Hz. The microphotographs (a) and (b) were taken at the time period 1 s, both at a high shutter speed 1/1000 s. Thin walls, seen on left and right sides of these micrographs, remain fixed confining the motion of the thick wall connected to the thin walls. (c) is a micrograph of the same objects as in micrographs (a) and (b) but taken at a slow shutter speed 1 s. This figure shows a thick-wall drift, averaged over a relatively long time period.

FIG. 9. (Color online) Sliding of zigzag walls in a chevron sample of the thickness $d = 5$ μm , for the voltage amplitude $U = 5$ V $< U_s$ and the frequency $f = 100$ Hz. The micrographs (a) and (b) were taken at the shutter speed 1/2000 s, in a time 1 s [(b) after (a)]. The arrows indicate an irreversible motion and a shortening of respective defect walls in this lapse of time.

FIG. 10. Experimental loss spectra obtained for a chevron system of the thickness $d = 5$ μm , in cases: $U = 0.3$ V $< U_1$ (\circ), $U_1 < U = 1.0$ V $< U_2$ (\triangle), and $U_2 < U = 5$ V $< U_s$ (\square). The shift of the maximum of ε'' in the case of $U = 5$ V gives evidence of nonlinear effects in collective azimuthal excitations of molecules.

TABLE I. Values of u_+ , ν , and f_{max} determined for chevron samples of different thicknesses. The parameters u_+ and ν were obtained by applying the procedure described in Sec. II and by using electro-optic data.

d [μm]	u_+ [m^{-1}]	ν	f_{max} [Hz]
5.0	6.95×10^4	0.348	1349.3
12.1	3.67×10^4	0.556	363.1
25.9	1.89×10^4	0.510	186.5
50.0	1.21×10^4	0.395	208.9

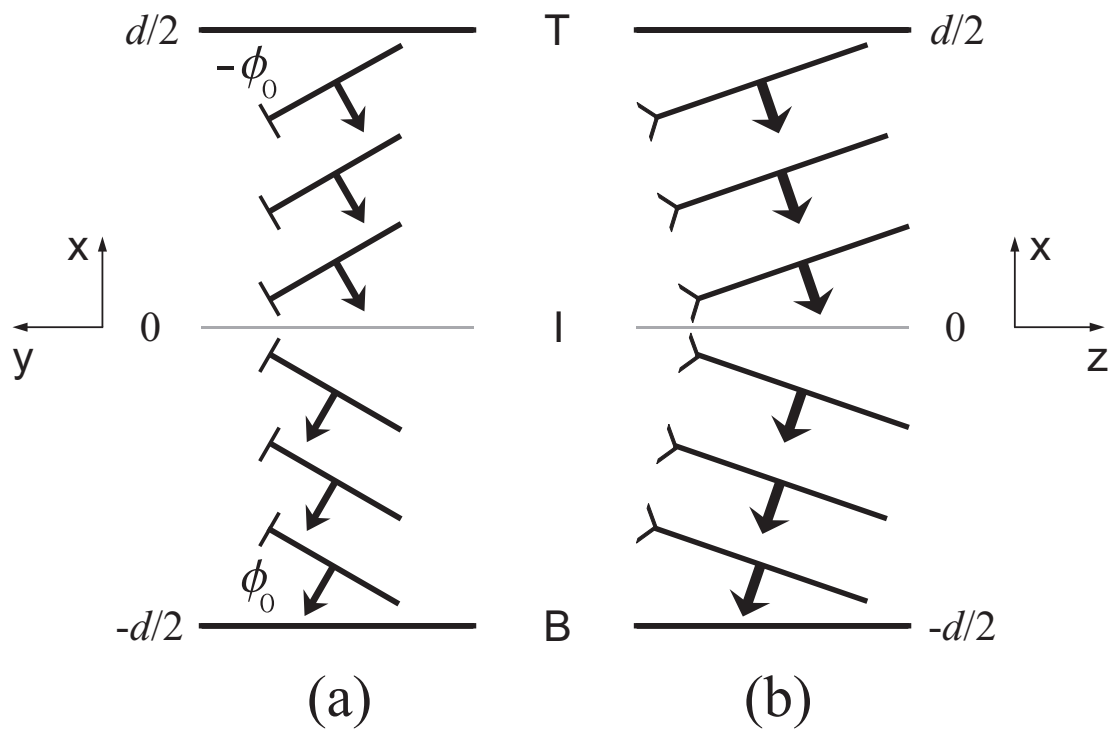


FIG. 1

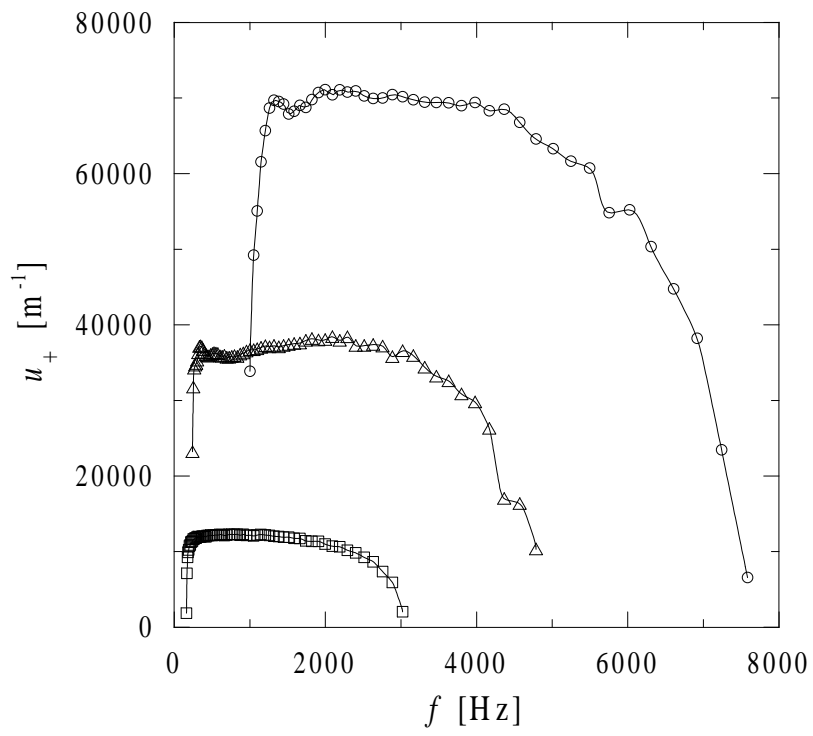


FIG. 2

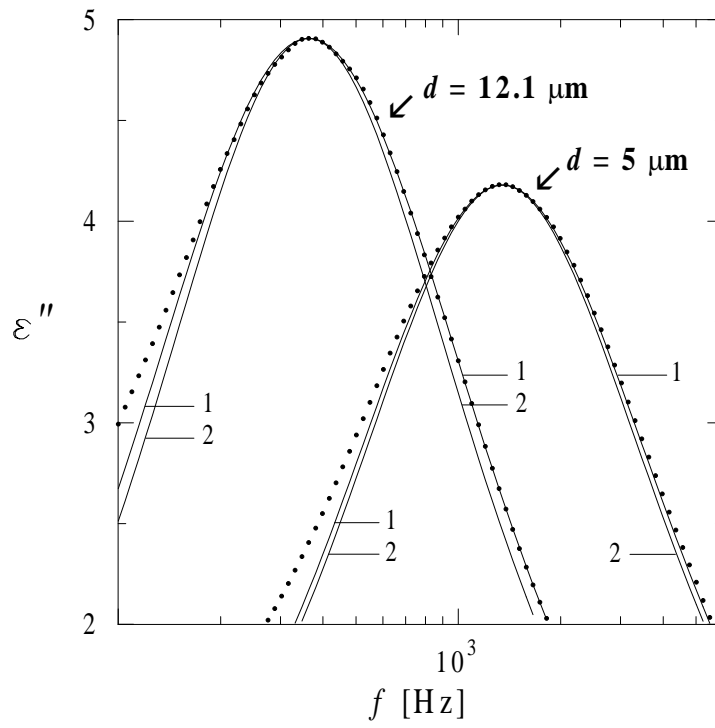


FIG. 3

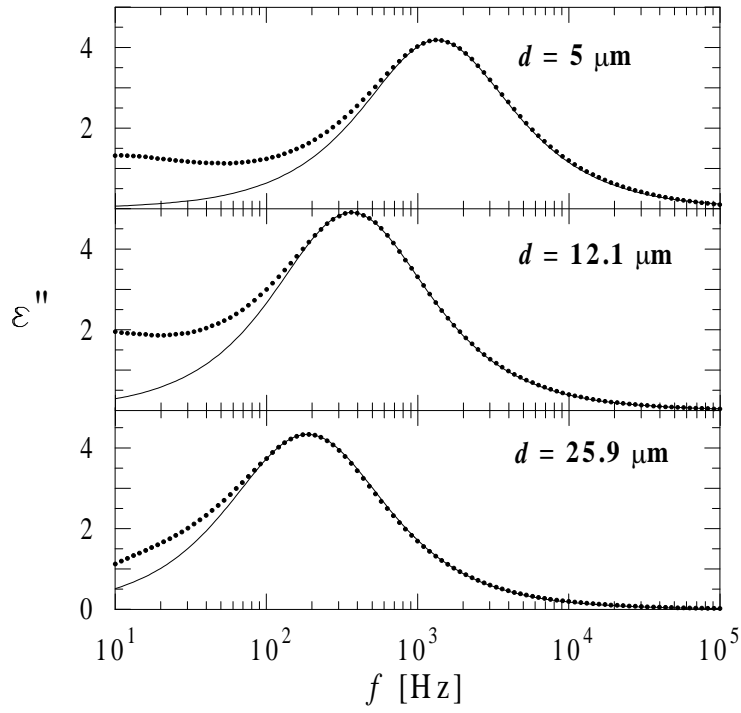


FIG. 4

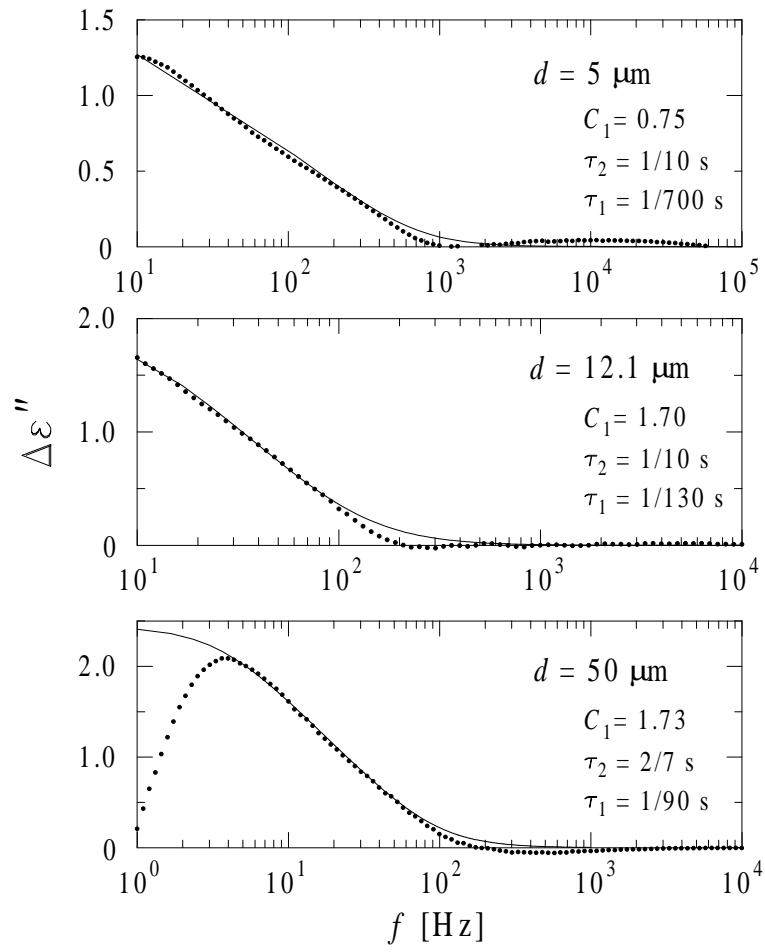


FIG. 5

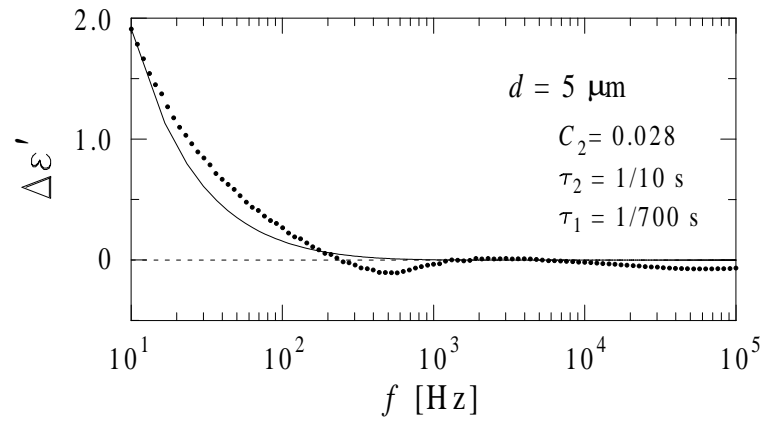


FIG. 6

This figure "FIG7.JPG" is available in "JPG" format from:

<http://arxiv.org/ps/cond-mat/0511103v4>

This figure "FIG8.JPG" is available in "JPG" format from:

<http://arxiv.org/ps/cond-mat/0511103v4>

This figure "FIG9.JPG" is available in "JPG" format from:

<http://arxiv.org/ps/cond-mat/0511103v4>

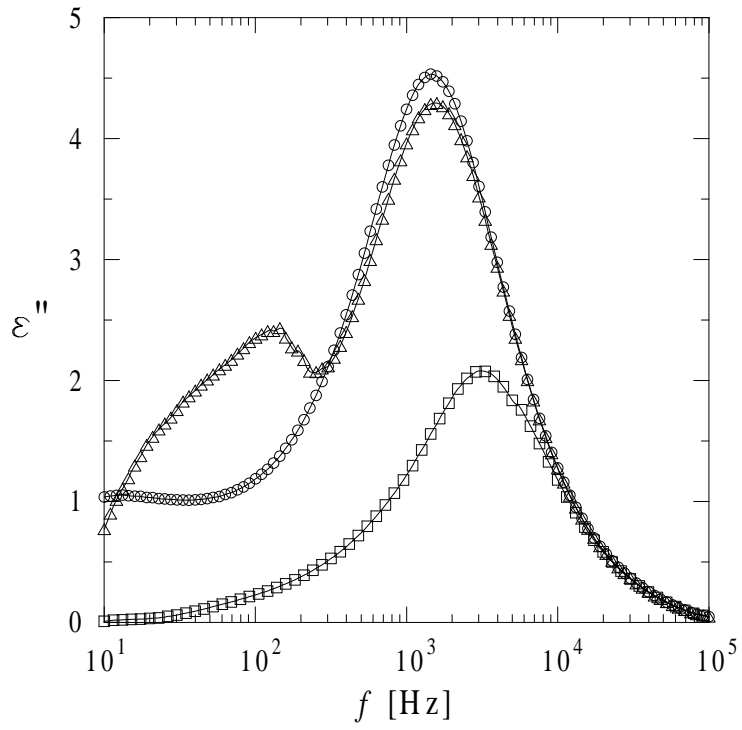


FIG. 10